



Cite this: *New J. Chem.*, 2019, 43, 18012

Received 3rd September 2019,
Accepted 17th October 2019

DOI: 10.1039/c9nj04544a

rsc.li/njc

“Off–on–off” type of selectively pH-sensing 8-hydroxyquinoline-substituted gallium(III) corrole†

Fangjian Cai,^{‡a} Fei Xia,^{‡b} Yingxin Guo,^a Weihua Zhu,^b Bo Fu,^{‡*a} Xu Liang,^{‡*bc} Shifa Wang,^{‡a} Zhengchun Cai^{‡a} and Haijun Xu^{‡*a}

We herein report the synthesis and pH-sensing properties of novel gallium corrole derivatives based on 8-hydroxyquinoline. The free base corrole and its gallium corrole derivatives were fully characterized using NMR spectroscopy and mass spectrometry. Their photophysical and electrochemical properties were also investigated using UV/Vis spectroscopy, fluorescence spectroscopy, MCD spectroscopy and cyclic voltammetry. A Ga-corrole derivative showed a good fluorescence response to change in pH in a wide pH range, from pH 1 to 12. Specifically, its fluorescence gradually diminished, from a high intensity at neutral pH, as the pH was either decreased or increased, *i.e.*, into acidic and basic conditions, respectively. These results indicated that the Ga-corrole derivative would be able to serve as an efficient “off–on–off” fluorescent sensor of pH in the solution state.

Introduction

The parameter pH is defined as the negative logarithm of hydrogen ion concentration, and is a critical target for a broad range of applications in diverse fields including biomedical, environmental, chemical and industrial fields.^{1–3} In particular, pH plays an extremely important role in physiological and pathological processes, such as cellular proliferation and apoptosis, enzyme activity, tumor multiplication and transport, muscle contraction, drug resistance, ion transport and homeostasis.^{4–6} A small pH change can destroy the activities of many plants and animals.^{5,7} An inappropriate intracellular pH level leads to a series of diseases in biological systems, such as cancers and Alzheimer's disease.^{8–10} Therefore, the measurement of pH is very important in these fields. Various analytical techniques such as UV-Vis absorption spectroscopy,¹¹ fluorescence spectroscopy,¹² Raman sensors,¹³ electrochemistry,¹⁴ and nuclear magnetic resonance¹⁵ have been used for determining pH values.

Among these methods, fluorescence-based techniques have attracted the most attention due to their superior properties

such as convenient operation, good spatial and temporal resolution, high selectivity, real-time detection, rapidity, high sensitivity and wide applicability.^{2,16,17} Furthermore, a wide range of fluorescent probes have been developed and applied to determine the pH in all kinds of environments.^{4,18} Many different kinds of organic fluorophores including rhodamine,¹⁹ BODIPY,^{20,21} fluoresceins,²² hemicyanine chromophore and coumarines^{23,24} have been used for the design of pH probes and have been widely studied.

In recent years, corroles have received a great deal of attention and have shown potential applications in the fields of field-effect transistors,^{7,25} electrochemistry,^{26–28} chemical sensors,^{29–32} catalytic systems,³³ electrochromic devices,³⁴ artificial photosynthesis,^{35,36} biomedical sensing and imaging^{37,38} and photodynamic therapy (PDT)^{39,40} owing to their unique photochemical and photosensitizing properties such as high radiative rate constants, large Stoke's shifts, absorption and emission bands in the visible region and high luminescence quantum yields.^{30,41,42} Among their metal complexes, Ga-corrole derivatives have shown particularly good application prospects in dye-sensitized solar cells, fluorescent probes, and the detection and tracking of tumors during cancer treatment.^{29,42,43} However, there have been few investigations on the use of Ga-corroles for pH sensing. Ga-corrole derivatives possess several advantages over the other sensor candidates such as easy synthesis and strong absorption of light in the visible region; they also show higher fluorescence quantum yields than that of zinc porphyrin. In addition, some of the pH probes based on protonation or deprotonation with heteroatom-containing groups such as pyridinyl, quinolyl, amino and phenol groups were designed to have a significant impact on the emission intensity or color

^a Jiangsu Co-Innovation Center of Efficient Processing and Utilization of Forest Resources, College of Chemical Engineering, Jiangsu Key Lab of Biomass-Based Green Fuels and Chemicals, Nanjing Forestry University, Nanjing 210037, P. R. China. E-mail: fubo@njfu.edu.cn, xuhaijun@njfu.edu.cn; Fax: +86-511-8879-1928; Tel: +86-511-8879-1928

^b School of Chemistry and Chemical Engineering, Jiangsu University, Zhenjiang 212013, P. R. China. E-mail: liangxu@ujs.edu.cn

^c State Key Laboratory of Coordination Chemistry, Nanjing University, Nanjing, 210000, P. R. China

† Electronic supplementary information (ESI) available. See DOI: 10.1039/c9nj04544a

‡ These authors equally contribute to this work.

of the chromophore.^{16,44,45} 8-Hydroxyquinoline, which contains pyridinyl and phenol units, has been extensively studied in recent years due to their impressive optical properties and excellent charge-transport properties.⁴⁶ However, despite the extensive investigations devoted to developing fluorescent sensors with the 8-hydroxyquinoline unit as the receptor for metal ions,^{47,48} only a few fluorescent pH sensors based on 8-hydroxyquinoline have been reported to the best of our knowledge.^{49–51} Therefore, the construction of Ga-corrole derivatives containing the 8-hydroxyquinoline moiety was expected to be of interest for the synthesis of pH sensor molecules with appealing protonation/deprotonation functionalities.

In the current work, we designed a new pH sensor molecule by combining Ga-corrole and 8-hydroxyquinoline moieties. The photophysical properties of this molecule were investigated, and proton titration experiments, HRMS, elemental analyses and NMR spectroscopy were performed on it. The fluorescence emission spectrum of this Ga-corrole derivative exhibited a remarkable dependence on pH in acidic and basic conditions. This derivative can thus be used as a highly sensitive “off-on-off” probe of pH.

Experimental

General

¹H NMR spectra were recorded using a Bruker AVANCE III 600M spectrometer. Chemical shifts for ¹H NMR spectra were expressed in parts per million (ppm) relative to CDCl₃ ($\delta = 7.26$ ppm) as the internal standard. UV-Vis spectra were recorded using a Shimadzu UV-2600 spectrophotometer at ambient temperature with a 1 cm quartz cell. MCD spectra were acquired using a JASCO-810 spectrometer with a permanent magnet (1.6 T). Elemental analyses for C, H and N were performed using a PerkinElmer 240C elemental analyzer. High-resolution mass spectroscopy (HRMS) data were collected using an LTQ Orbitrap XL spectrometer equipped with an electrospray ionization (ESI) source. Cyclic voltammetry was performed with a three-electrode-compartment cell in *o*-dichlorobenzene (*o*-DCB) solutions with 0.1 M [*n*-Bu₄N](ClO₄) as the supporting electrolyte using a CHI-730D electrochemistry workstation. A glassy carbon electrode with a diameter of 3 mm was used as the working electrode, while platinum wire and Ag/AgCl electrodes were used as the counter and reference electrodes, respectively. 5-Pentafluorophenyl-dipyrrromethane was synthesized according to the literature.⁵² 8-Hydroxyquinoline-2-carbaldehyde was synthesized according to the literature.⁵³

Synthesis of H₃ corrole 1. 5-(Pentafluorophenyl)-dipyrrromethane (1.75 g, 6.0 mmol) and 8-hydroxyquinoline-2-carbaldehyde (0.346 g, 2.0 mmol) were dissolved in dry CH₂Cl₂ (160 mL) under an argon atmosphere. The resulting mixture was shielded from light, and TFA (40 μ L) was added slowly to it at room temperature. The resulting reaction mixture was stirred for 4 h, and then diluted with 600 mL of CH₂Cl₂. At this point, DDQ (1.73 g, 7.62 mmol) was added to the diluted mixture, and the stirring was continued at room temperature overnight.

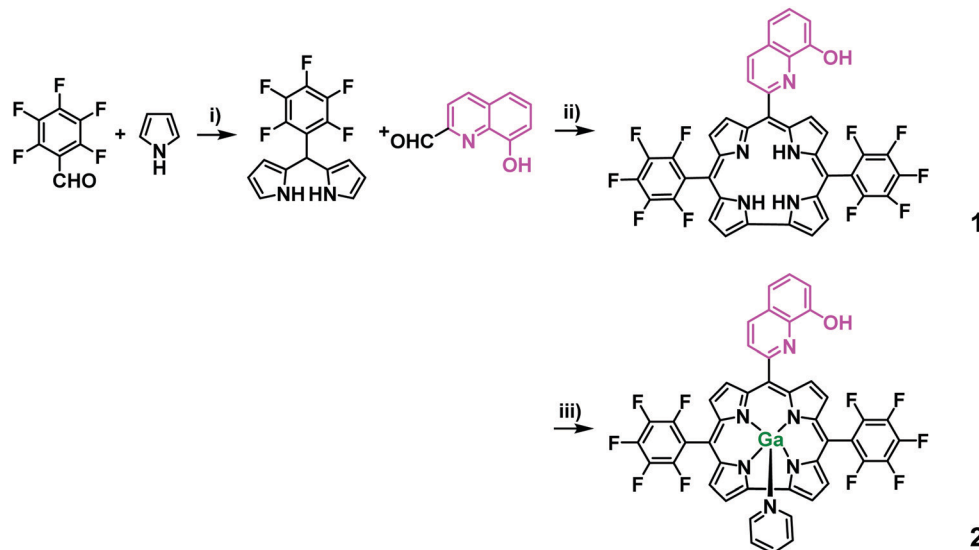
The resulting mixture was neutralized with triethylamine (1.0 mL). The solvent was removed under reduced pressure, and the residue was purified by column chromatography and on silica gel with 50% DCM-petroleum ether as eluent to afford the title compound in 16% yield (315.0 mg). UV-Vis (CH₂Cl₂), $\lambda_{\text{max}}/\text{nm}$ [$\epsilon \times 10^{-5}/(\text{L mol}^{-1} \text{cm}^{-1})$]: 426 (0.8608), 568 (0.1165), 610 (0.0923), 662 (0.0572); ¹H NMR (CDCl₃, 600 MHz, ppm) δ 9.13 (d, ³*J*_{H-H} = 3.6 Hz, 2H), 8.60 (s, 4H), 8.56 (d, ³*J*_{H-H} = 1.8 Hz, 2H), 8.44–8.57 (m, 2H), 7.64–7.68 (m, 2H), 7.41 (d, ³*J*_{H-H} = 12 Hz, 1H). HRMS (ESI): *m/z* calc'd for C₄₀H₁₆F₁₀N₅O [M – H][–]: 772.1195; found: 772.1182. Elemental analysis calc'd (%) for C₄₀H₁₇F₁₀N₅O: C 62.10, H 2.22, N 9.05; found: C 62.04, H 2.12, N 9.13.

Synthesis of Ga(III) corrole 2. A solution of 1 (77.4 mg, 0.1 mmol) and gallium chloride (0.176 g, 1.0 mmol) in pyridine (20 mL) was stirred and refluxed at 140 °C for 2 h. The resultant solution was evaporated, and the crude product was purified by column chromatography with silica gel, and eluted with petroleum ether/CH₂Cl₂. After removal of the solvents, the solid was recrystallized from THF/petroleum ether (1 : 5). 2 was obtained as a black solid in a yield of 40% (37 mg, based on the ligand). UV-Vis (CH₂Cl₂), $\lambda_{\text{max}}/\text{nm}$ [$\epsilon \times 10^{-5}/(\text{L mol}^{-1} \text{cm}^{-1})$]: 419 (1.333), 480 (0.1493), 519 (0.2652), 572 (0.1029), 596 (0.0966), 642 (0.0836); ¹H NMR (CDCl₃, 600 MHz, ppm) δ 9.25 (d, ³*J*_{H-H} = 3.6 Hz, 2H), 8.89 (m, 4H), 8.82 (d, ³*J*_{H-H} = 3.6 Hz, 2H), 8.60 (s, 2H), 8.50–8.37 (m, 2H), 8.69–8.64 (m, 2H), 7.40 (d, ³*J*_{H-H} = 1.2 Hz, 1H), 6.92 (m, 3H), 6.23 (m, 2H), 4.38 (d, ³*J*_{H-H} = 0.6 Hz, 1H). HRMS (ESI): *m/z* calc'd for C₄₅H₂₀F₁₀GaN₆O [M + H]⁺: 919.0789; found: 919.0801. Elemental analysis calc'd (%) for C₄₅H₁₉F₁₀GaN₆O: C 58.79, H 2.08, N 9.14; found: C 58.68, H 2.12, N 9.08.

Results and discussion

Synthesis and structural characterization

The synthetic route used to prepare the Ga(III) corrole derivative 2 is given in Scheme 1. The free base corrole 1 and Ga-corrole 2 were synthesized according to procedures described in the literature.^{40,54–57} 8-Hydroxyquinoline-2-carbaldehyde was reacted with 2,2'-(perfluorophenyl)methylenebis(1*H*-pyrrole) in dry CH₂Cl₂ in the presence of a catalytic amount of trifluoroacetic acid for 4 h under argon, followed by oxidation with 2,3-dichloro-5,6-dicyano-1,4-benzoquinone (DDQ). Repeated purification by silica gel column chromatography gave 1 in 16% yield as the only isolable product. The free corrole (1) precursor was reacted with excess dried GaCl₃ in dry pyridine to give the metalated compound 2 in 40% yield. The structures of the new compounds were also characterized using high-resolution mass spectrometry (HRMS) and ¹H NMR spectroscopy (Fig. S1–S4, see ESI†). The ¹H NMR spectrum of compound 1 showed eight signals ascribed to the β -protons in the range 8.58–9.13 ppm. The ¹H NMR spectrum of 2 shows three signals due to the pyrrolic β -protons at 9.23, 8.86, and 8.80 ppm. The *para*-, *ortho*- and *meta*-pyridine protons appeared at 6.90, 6.21 and 4.36 ppm. The chemical shifts of the *para*-, *ortho*- and *meta*-¹⁹F NMR resonances of compound 2 occur at



Scheme 1 Procedure used to synthesize the target compound. (i) TFA, DCM, (ii) a. TFA, DCM, Ar, b. DDQ, and (iii) GaCl₃, pyridine.

–139.12, –155.35 and –163.19 ppm, respectively. HRMS-electrospray ionization (HRMS-ESI) revealed parent ion peaks at $m/z = 772.1182$ (calculated for C₄₀H₁₆F₁₀N₅O: 772.1195 [M – H]⁺) for compound **1** and 919.0789 (calculated for C₄₅H₂₀F₁₀GaN₆O: 919.0801 [M + H]⁺) for compound **2**.

Electronic structure

The photophysical properties of compounds **1** and **2** were investigated using UV-vis absorption spectrophotometry as well as steady-state and time-resolved fluorescence spectroscopy in CH₂Cl₂. The steady-state absorption and normalized fluorescence spectra of compounds **1–2** in CH₂Cl₂ are shown in ESI† (Fig. S5 and S6). Their photophysical data are summarized in Table 1. As shown in Fig. S5 (ESI†), free-base corrole **1** yielded a typical Soret band at a wavelength of 426 nm and Q bands at 568, 610, and 662 nm. In comparison with the free-base corrole **1**, gallium corrole **2** exhibited more intense absorptions at both Soret (419 nm) and Q bands (572 nm, 596 nm, 642 nm), accompanied by blue shifts. The emission spectra of both compounds **1** and **2** were also recorded in CH₂Cl₂ solutions (Fig. S6, see ESI†) and presented essentially perfect mirror-image relationships with their Q-like bands. The introduction of gallium into the corrole core resulted in blue shifts of the fluorescence emission, and the fluorescence emission maxima for **1** and **2** were centered at 640 nm and 603 nm, respectively. However, Ga-corrole **2** exhibited comparably good fluorescence intensities as indicated by a quantum yield of 12%, while free base corrole **1** showed poor fluorescence intensities with a quantum yield of 6% (Table 1). In addition, fluorescence

lifetime (τ) values of compounds **1** and **2** were determined from time-resolved fluorescence spectroscopy data, which showed single exponential decays with lifetimes of 4.06 ns and 2.42 ns (Table 1), respectively. The radiative decay rate constant (k_r) values and nonradiative decay rate constant (k_{nr}) values of compounds **1** and **2** were determined from the fluorescence lifetime (τ_f) values and quantum yield (Φ_f) values using the equations $k_r = \Phi_f/\tau$ and $k_{nr} = (1 - \Phi_f)/\tau$, respectively, and are summarized in Table 1. Compound **2** showed higher k_r and k_{nr} values than those of **1**. These results are very similar to the previously reported data obtained on corroles and gallium(III) corroles.^{58–61}

Magnetic circular dichroism (MCD) spectra can be analyzed on the basis of the three Faraday terms.¹⁴ The low symmetry of the corroles dictated that only Faraday B₀ terms were here observed (Fig. 1). In this context, Michl's perimeter model¹² was used together with MCD spectroscopy to analyze the properties of the corrole π -system.^{13,14} The –+ shape sign sequence in ascending energy terms observed for the Faraday B₀ terms in the Q band region of the MCD spectra clearly identified a weak shoulder of intensity at ca. 624 nm to the red side of the main absorption band at ca. 602, and identified 575 nm as also being electronic in origin due to the symmetry-induced split of the Q band absorptions. This pattern is typically observed for corroles, since the separation of the MOs derived from the LUMO of the parent perimeter (referred to as the Δ LUMO value to use Michl's terminology¹²) is greater than that of those derived from the HOMO level (the Δ HOMO value). As would normally be anticipated, a –+ sign sequence was also identified for the main bands in the B region. A weak

Table 1 The emission spectra data of compounds **1** and **2** in CH₂Cl₂

Compounds	$\lambda_{\text{abs}}/\text{nm}$ ($\epsilon \times 10^4 \text{ M}^{-1} \text{ cm}^{-1}$)	λ_{em} (nm)	Φ_f	τ_f [ns]	$\Delta\mu$ (nm)	k_r [10^8 s^{-1}]	k_{nr} [10^8 s^{-1}]
1	426 (86.08), 568 (11.65), 610 (9.23), 662 (5.72)	640	5.74	4.06	230	0.1414	2.3217
2	419 (133.33), 480 (14.93), 519 (26.52), 572 (10.29), 596 (9.66), 642 (8.36)	603	11.7	2.42	198	0.4835	3.6488

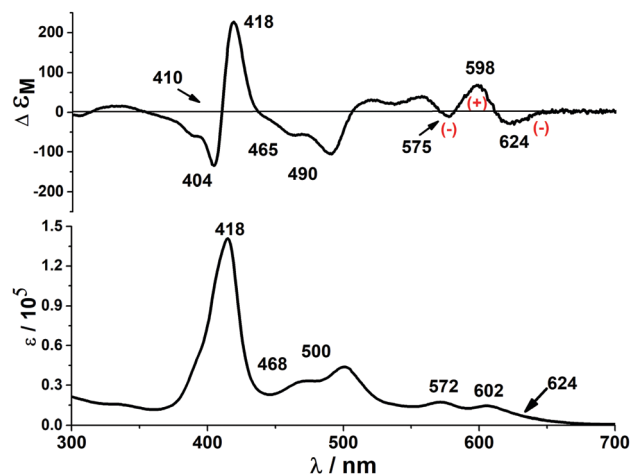


Fig. 1 UV-vis absorption (bottom) and magnetic circular dichroism (MCD) (top) spectra of Ga(III) corrole **2** in THF.

shoulder of intensity at about 420 nm can be assigned to the symmetry-induced splitting of the B bands into *x*- and *y*-polarized components. The complex sequence of bands of Ga(III) corrole **2** that are observed in this region is consistent with the presence of both $\pi\pi^*$ and ligand-to-metal charge transfer (LMCT) bands between the Soret and Q band regions. In order to better understand the electronic structure of Ga(III) corrole **2**, it was also electrochemically characterized, and its $E_{1/2}$ values were derived from both CV and DPV analyses (Fig. S7, see ESI†). The Ga(III) corrole **2** showed a reversible ring oxidation and reduction at $E_{1/2} = 1.15$ and -1.34 V, respectively. Also, a quasi-reversible process appeared at $E_{1/2} = -0.92$ V, which was assigned as the reduction of gallium ions and the removal of pyridine ligands.

Selective pH sensors

To test the applicability of compound **2** as a selective probe of pH, we further investigated the pH-dependent photophysical properties of **2** with the 8-hydroxyquinolyl moiety. Upon addition of various ions including Na^+ , K^+ , Mg^{2+} , Mn^{2+} , Fe^{2+} , Cu^{2+} , Ni^{2+} , Cr^{3+} , Co^{2+} , Cd^{2+} , and Zn^{2+} into respective samples of a mixed solvent of H_2O and CH_3CN ($v/v = 1:9$), few to no changes were observed that indicated the minor cation effect on the fluorescence spectra (Fig. S8, see ESI†). The pH titration experiments were carried out in a mixed solvent of H_2O and CH_3CN ($v/v = 1:9$) upon addition of trifluoroacetic acid (TFA) for protonation of pyridyl N atom of 8-hydroxyquinolyl group and NaOH used for deprotonation of the $-\text{OH}$ group, respectively. It should be mentioned here that the solution color and spectral properties resulted in few to no changes in any of the measurements. In contrast, the fluorescence intensity of **2** under acidic conditions gradually decreased as the pH was decreased from 6.45 to 0.95, and no obvious spectral shift was observed during the whole titration, as seen in Fig. 2. When a large amount of TFA was added, the fluorescence was quenched completely. This observation suggested that a new species was formed as a result of the protonation of N atoms in the pyridine

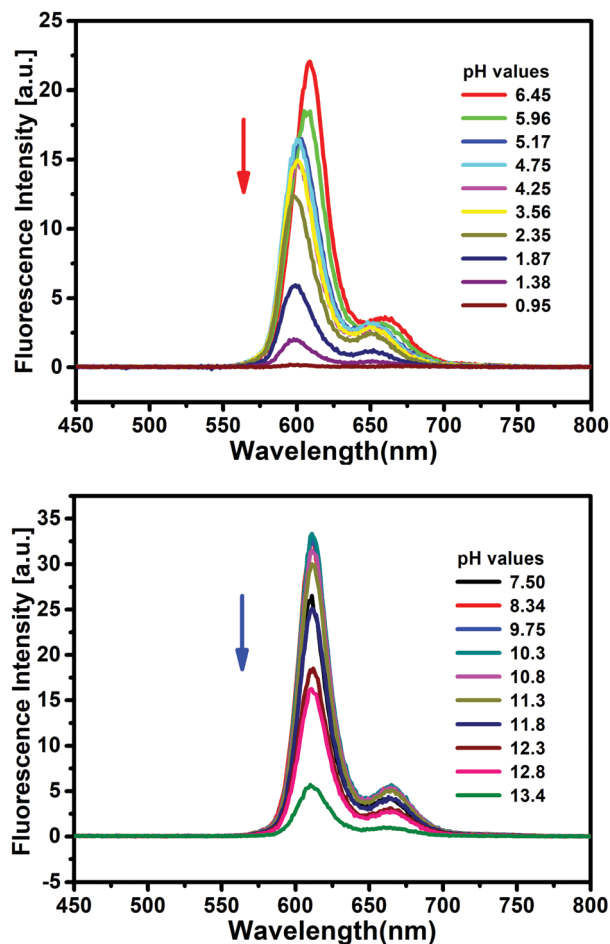


Fig. 2 Fluorescence emission spectra of 1.25×10^{-5} M Ga(III) corrole **2** at various acidic (top) and basic conditions (bottom) in a mixed solvent of H_2O and CH_3CN (1:9) with an excitation wavelength of 500 nm.

group, which resulted in a photoinduced electron transfer (PET) quenching process.⁵³ In addition, as shown in Fig. 2, as the pH was increased from 7.50 to 13.4, the fluorescence intensity of **2** under basic conditions also gradually diminished in a similar manner as was observed under acidic conditions. This observation was attributed to the phenol moiety of 8-hydroxyquinoline being sensitive to the environmental pH and being easily deprotonated to form a phenolate anion under basic conditions, and the electron-rich substituents are able to quench the fluorescence of Ga(III) corrole due to the photoinduced electron transfer process.²¹ The dependence of the fluorescence intensity of **2** on pH is an example of an “off-on-off” mechanism. These obtained results suggested that a photoinduced electron transfer (PET) quenching process between the 8-hydroxyquinoline receptor and corrole-Ga fluorescence signal unit was responsible for the observed dependence of the fluorescence of **2** on pH in our experiments with different pH values from 6.45 to 0.95 and 7.50 to 13.4, consistent with the reported literature.⁵³ Herein, the remarkable changes of fluorescence intensity during the pH titrations implied that compound **2** could be used as a highly sensitive probe for detecting pH changes under both acidic and basic conditions. In addition, to understand how the pH probe

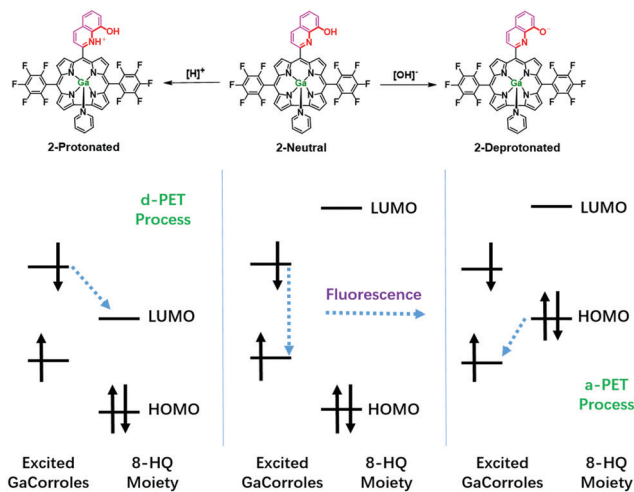


Fig. 3 Proposed mechanism of the photoinduced electron transfer between the Ga(III) corrole moiety and 8-HQ unit of compound **2** in protonated quinolinium, neutral, and deprotonated quinolate states, respectively.

works, a PET quenching mechanism involving the orbital energy levels of the excited states of the Ga(III) corrole moiety and 8-HQ unit was proposed with compound **2** as an example, as shown in Fig. 3. In principle, Ga(III) corrole upon photoexcitation can serve as both an electron donor and acceptor. In other words, the photoinduced electron can move from the excited Ga-corrole moiety to the lowest unoccupied molecular orbital (LUMO) of 8-HQ (donor-excited PET; d-PET) or move in sort of an opposite direction, namely from the highest occupied molecular orbital (HOMO) of 8-HQ to the excited Ga-corrole moiety (acceptor-excited PET; a-PET).

Conclusions

In this work, the low-symmetry A_2B -type free base corrole and its gallium corrole derivatives with 8-hydroxyquinoline were successfully synthesized, isolated and fully characterized using NMR spectroscopy and mass spectrometry. Their photophysical and electrochemical properties were also investigated using UV/Vis spectroscopy, fluorescence spectroscopy, MCD spectroscopy and cyclic voltammetry. The Ga-corrole derivative showed a good fluorescence response to changes in pH in a wide pH region of 1 to 14. Its fluorescence, observed to be relatively intense at neutral pH conditions, became gradually weaker as the pH was either decreased (*i.e.*, as the conditions became more acidic) or increased (*i.e.*, as the conditions became more basic). These results indicated that the Ga-corrole derivative would be able to serve as an efficient “off-on-off” fluorescent pH sensor in the solution state. Also, a plausible mechanism for the fluorescence response was proposed.

Conflicts of interest

There are no conflicts to declare.

Acknowledgements

This work was supported by National Key R&D Program of China (2016YFD0600804), the National Natural Science Foundation of China (21701058, 21301092 and 21703086), the Natural Science Foundation of Jiangsu province (BK20160922 and BK20160499), the State Key Laboratory of Coordination Chemistry (projects SKLCC1817), the China Post-doc Foundation (No. 2018M642183), the Lanzhou High Talent Innovation and Entrepreneurship Project (No. 2018-RC-105) and Jiangsu University (17JDG035, X. L.).

Notes and references

- J. Mandal, P. Ghorai, P. Brandão, K. Pal, P. Karmakar and A. Saha, *New J. Chem.*, 2018, **42**, 19818–19826.
- C. Yuan, J. Li, H. Xi and Y. Li, *Mater. Lett.*, 2019, **236**, 9–12.
- Z. L. Wu, M. X. Gao, T. T. Wang, X. Y. Wan, L. L. Zheng and C. Z. Huang, *Nanoscale*, 2014, **6**, 3868–3874.
- J. Yin, Y. Hu and J. Yoon, *Chem. Soc. Rev.*, 2015, **44**, 4619–4644.
- R. Bag, Y. Sikdar, S. Sahu, D. K. Maiti, A. Frontera, A. Bauza, M. G. B. Drew and S. Goswami, *Dalton Trans.*, 2018, **47**, 17077–17085.
- Y. Ning, X. Wang, K. Sheng, L. Yang, W. Han, C. Xiao, J. Li, Y. Zhang and S. Wu, *New J. Chem.*, 2018, **42**, 14510–14516.
- M. Li, W. Yang, P. Qiu, G. Ren, C. Li, Z. Chen, Y. Wang and Q. Pan, *J. Lumin.*, 2019, **205**, 380–384.
- A. L. Edinger and C. B. Thompson, *Curr. Opin. Cell Biol.*, 2004, **16**, 663–669.
- S. Bhuniya, S. Maiti, E. J. Kim, H. Lee, J. L. Sessler, K. S. Hong and J. S. Kim, *Angew. Chem., Int. Ed.*, 2014, **53**, 4469–4474.
- X. Yue, C. O. Yanez, S. Yao and K. D. Belfield, *J. Am. Chem. Soc.*, 2013, **135**, 2112–2115.
- A. Mitra, S. Bose, S. Biswas, P. Bandyopadhyay and A. Sarkar, *ChemPlusChem*, 2018, **83**, 832–837.
- Z. Wang, Y. Zhang, M. Li, Y. Yang, X. Xu, H. Xu, J. Liu, H. Fang and S. Wang, *Tetrahedron*, 2018, **74**, 3030–3037.
- J. Wang, Y. Geng, Y. Shen, W. Shi, W. Xu and S. Xu, *Sens. Actuators, B*, 2019, **290**, 527–534.
- J. Zhou, L. Zhang and Y. Tian, *Anal. Chem.*, 2016, **88**, 2113–2118.
- S. Hesse, G. Ruijter, C. Dijkema and J. Visser, *J. Biotechnol.*, 2000, **77**, 5–15.
- A. I. Said, N. I. Georgiev and V. B. Bojinov, *Dyes Pigm.*, 2019, **162**, 377–384.
- Z. Bai, R. Chen, P. Si, Y. Huang, H. Sun and D. H. Kim, *ACS Appl. Mater. Interfaces*, 2013, **5**, 5856–5860.
- D. Wencel, T. Abel and C. McDonagh, *Anal. Chem.*, 2014, **86**, 15–29.
- G. Bao, K. L. Wong and P. A. Tanner, *ChemPlusChem*, 2019, **84**, 816–820.
- L. Gai, J. Mack, H. Lu, H. Yamada, D. Kuzuhara, G. Lai, Z. Li and Z. Shen, *Chem. – Eur. J.*, 2014, **20**, 1091–1102.

- 21 J. Qiu, S. Jiang, H. Guo and F. Yang, *Dyes Pigm.*, 2018, **157**, 351–358.
- 22 F. Y. Ge and L. G. Chen, *J. Fluoresc.*, 2008, **18**, 741–747.
- 23 X. Li, Y. Yue, Y. Wen, C. Yin and F. Huo, *Dyes Pigm.*, 2016, **134**, 291–296.
- 24 L. Long, Y. Wu, L. Wang, A. Gong, R. Hu and C. Zhang, *Anal. Chim. Acta*, 2016, **908**, 1–7.
- 25 T. Rantanen, M.-L. Järvenpää, J. Vuojola, K. Kuningas and T. Soukka, *Angew. Chem., Int. Ed.*, 2008, **120**, 3871–3873.
- 26 V. Quesneau, W. Shan, N. Desbois, S. Brandès, Y. Rousselin, M. Vanotti, V. Blondeau-Patissier, M. Naitana, P. Fleurat-Lessard, E. V. Caemelbecke, K. M. Kadish and C. P. Gros, *Eur. J. Inorg. Chem.*, 2018, 4265–4277.
- 27 X. Jiang, M. L. Naitana, N. Desbois, V. Quesneau, S. Brandès, Y. Rousselin, W. Shan, W. R. Osterloh, V. Blondeau-Patissier, C. P. Gros and K. M. Kadish, *Inorg. Chem.*, 2018, **57**, 1226–1241.
- 28 X. Jiang, W. Shan, N. Desbois, V. Quesneau, S. Brandès, E. Van Caemelbecke, W. R. Osterloh, V. Blondeau-Patissier, C. P. Gros and K. M. Kadish, *New J. Chem.*, 2018, **42**, 8220–8229.
- 29 C. I. M. Santos, E. Oliveira, J. F. B. Barata, M. A. F. Faustino, J. A. S. Cavaleiro, M. G. P. M. S. Neves and C. Lodeiro, *Inorg. Chim. Acta*, 2014, **417**, 148–154.
- 30 C. L. He, F. L. Ren, X. B. Zhang and Z. X. Han, *Talanta*, 2006, **70**, 364–369.
- 31 A. Savoldelli, G. Magna, C. Di Natale, A. Catini, S. Nardis, F. R. Fronczek, K. M. Smith and R. Paolesse, *Chem. – Eur. J.*, 2017, **23**, 14819–14826.
- 32 S. Brandès, V. Quesneau, O. Fonquernie, N. Desbois, V. Blondeau-Patissier and C. P. Gros, *Dalton Trans.*, 2019, **48**, 11651–11662.
- 33 L. T. Huang, A. Ali, H. H. Wang, F. Cheng and H. Y. Liu, *J. Mol. Catal. A: Chem.*, 2017, **426**, 213–222.
- 34 Y. Fang, Z. Ou and K. M. Kadish, *Chem. Rev.*, 2017, **117**, 3377–3419.
- 35 B. Liu, H. Fang, X. Li, W. Cai, L. Bao, M. Rudolf, F. Plass, L. Fan, X. Lu and D. M. Guldi, *Chem. – Eur. J.*, 2015, **21**, 746–752.
- 36 J. Yang, F. J. Cai, X. M. Yuan, T. Meng, G. X. Xin, S. F. Wang, C. P. Gros and H. J. Xu, *J. Porphyrins Phthalocyanines*, 2018, **22**, 777–783.
- 37 H. Agadjanian, J. Ma, A. Rentsendorj, V. Valluripalli, J. Y. Hwang, A. Mahammed, D. L. Farkas, H. B. Gray, Z. Gross and L. K. Medina-Kauwe, *Proc. Natl. Acad. Sci. U. S. A.*, 2009, **106**, 6105–6110.
- 38 A. Kanamori, M. M. Catrinescu, A. Mahammed, Z. Gross and L. A. Levin, *J. Neurochem.*, 2010, **114**, 488–498.
- 39 R. D. Teo, J. Y. Hwang, J. Termini, Z. Gross and H. B. Gray, *Chem. Rev.*, 2017, **117**, 2711–2729.
- 40 Z. Zhang, H. H. Wang, H. J. Yu, Y. Z. Xiong, H. T. Zhang, L. N. Ji and H. Y. Liu, *Dalton Trans.*, 2017, **46**, 9481–9490.
- 41 I. Aviv-Harel and Z. Gross, *Chem. – Eur. J.*, 2009, **15**, 8382–8394.
- 42 J. F. Barata, M. G. Neves, M. A. Faustino, A. C. Tome and J. A. Cavaleiro, *Chem. Rev.*, 2017, **117**, 3192–3253.
- 43 R. Mishra, B. Basumatary, R. Singhal, G. D. Sharma and J. Sankar, *ACS Appl. Mater. Interfaces*, 2018, **10**, 31462–31471.
- 44 N. Tuncer, E. Teknikel and C. Unaleroğlu, *J. Fluoresc.*, 2018, **28**, 1413–1420.
- 45 T. Gong, W. Yang, M. Zhang, W. Zhou and R. Xue, *J. Mater. Sci.*, 2018, **53**, 13900–13911.
- 46 X. Yu, X. Jin, G. Tang, J. Zhou, W. Zhang, J. Hu, Q. Xie and C. Zhong, *Appl. Organomet. Chem.*, 2013, **27**, 479–485.
- 47 X. H. Jiang, B. D. Wang, Z. Y. Yang, Y. C. Liu, T. R. Li and Z. C. Liu, *Inorg. Chem. Commun.*, 2011, **14**, 1224–1227.
- 48 J. Wang, L. Long, D. Xie and X. Song, *Sens. Actuators, B*, 2013, **177**, 27–33.
- 49 Y. Chen, H. Wang, L. Wan, Y. Bian and J. Jiang, *J. Org. Chem.*, 2011, **76**, 3774–3781.
- 50 L. Chen, L. He, F. Ma, W. Liu, Y. Wang, M. A. Silver, L. Chen, L. Zhu, D. Gui, J. Diwu, Z. Chai and S. Wang, *ACS Appl. Mater. Interfaces*, 2018, **10**, 15364–15368.
- 51 S. Kappaun, T. Sovic, F. Stelzer, A. Pogantsch, E. Zojer and C. Slugovc, *Org. Biomol. Chem.*, 2006, **4**, 1503–1511.
- 52 C. M. Lemon, R. L. Halbach, M. Huynh and D. G. Nocera, *Inorg. Chem.*, 2015, **54**, 2713–2725.
- 53 V. Chandrasekhar, S. Hossain, S. Das, S. Biswas and J. P. Sutter, *Inorg. Chem.*, 2013, **52**, 6346–6353.
- 54 A. Langlois, H. J. Xu, P. L. Karsenti, C. P. Gros and P. D. Harvey, *Chem. – Eur. J.*, 2017, **23**, 5010–5022.
- 55 J. M. Barbe, G. Canard, S. Brandes and R. Guillard, *Eur. J. Org. Chem.*, 2005, 4601–4611.
- 56 B. Brizet, N. Desbois, A. Bonnot, A. Langlois, A. Dubois, J.-M. Barbe, C. P. Gros, C. Goze, F. Denat and P. D. Harvey, *Inorg. Chem.*, 2014, **53**, 3392–3403.
- 57 F. Cheng, L. Huang, H. Wang, Y. Liu, J. Kandhadi, H. Wang, L. Ji and H. Y. Liu, *Chin. J. Chem.*, 2017, **35**, 86–92.
- 58 L. Shi, H. F. Jiang, W. Yin, H. H. Wang, H. Wang, L. Zhang, L. N. Ji and H. Y. Jiang, *Acta Phys. – Chim. Sin.*, 2012, **28**, 465–469.
- 59 D. Kowalska, X. Liu, U. Tripathy, A. Mahammed, Z. Gross, S. Hirayama and R. P. Steer, *Inorg. Chem.*, 2009, **48**, 2670–2676.
- 60 W. L. Shao, H. Wang, S. He, L. Shi, K. M. Peng, Y. F. Lin, L. Zhang, L. N. Ji and H. Y. Liu, *J. Phys. Chem. B*, 2012, **116**, 14228–14234.
- 61 F. Cheng, H. H. Wang, A. Ali, J. Kandhadi, H. Wang, X. L. Wang and H. Y. Liu, *J. Porphyrins phthalocyanines*, 2018, **22**, 1–13.